Fast protons and alpha particles from the $^{12}C+^{60}Ni$ reaction

R. L. Robinson, R. L. Auble, I. Y. Lee, M. J. Martin, G. R. Young, J. Gomez del Campo, J.B. Ball, F. E. Bertrand, R. L. Ferguson, C. B. Fulmer, and J. R. Wu*
Oak Ridge National Laboratory, Oak Ridge, Tennessee 37830

J. C. Wells
Tennessee Technological University, Cookeville, Tennessee 38501
and Oak Ridge National Laboratory, Oak Ridge, Tennessee 37830

H. Yamada
Vanderbilt University, Nashville, Tennessee 37235
(Received 17 July 1981)

The emission of energetic light ions from heavy-ion induced reactions was studied by measuring coincidences of protons and alpha particles with (1) $Z=1$ to 7 particles, (2) discrete γ rays, and (3) γ-ray multiplicities from bombardment of ^{60}Ni with ^{12}C ions. Incident beam energies were 136 and 194 MeV. Discrete γ rays were used to identify the residual targetlike fragments. Most of the particle-particle coincident angular correlations are strongly peaked in the forward direction; the full widths at half maximum of the proton distributions are typically 50°, those of the alpha particles are 30°. The N-Z distributions of the residual nuclei peak around ^{60}Ni. The γ-ray multiplicities are insensitive to the energy of the gating energetic light ion and are about 9 for 136-MeV ^{12}C projectiles and 10 for 194 MeV. The results indicate the contribution of more than one mechanism in producing the high-energy light ions. In part the energetic light ions are emitted in association with a projectilelike fragment. A major component of the energetic light ions can be explained as emission from the projectilelike fragment during the collision process followed by fusion of the remainder of the fragment with the target.

[NUCLEAR REACTIONS $^{60}Ni(^{12}C,p)$, $(^{12}C,\alpha)$ $E=136$, 194 MeV; measured $\sigma(E,\theta)$ in coincidence with $Z=1-6$ particles, γ rays and γ multiplicities.]

I. INTRODUCTION

It has been suggested[1] that for reactions induced with heavy-ion projectiles with energies of less than 10 MeV/nucleon, the duration of the collision is much longer than the transit time across the nucleus for a nucleon at the Fermi level, and the dominant phenomena are characteristic of the mean field. For projectiles with energy in excess of 200 MeV/nucleon, the reaction would be expected to proceed by independent collisions of the constituent particles. The metamorphosis between these two extremes is little studied and poorly understood. For heavy ions with energies between these two limits, the resulting energy spectra of $Z=1,2$ particles have high-energy components which extend far beyond that expected for particle evaporation from an equilibrated system following fusion of the target and projectile. Investigation of these nonequilibrium light ions provides an important method of exploring the reaction mechanisms in this intermediate region.

The inclusive spectra of the energetic light ions are characterized by strong peaking in the forward direction and an approximately exponential decrease in yield with increasing energy of the emitted light ions. Several models provide reasonable fits to the simple dependence of the inclusive light-ion spectra on laboratory energy and angle. Symons *et al.*[2] were able to fit proton spectra resulting from bombardment of ^{197}Au with 315-MeV ^{16}O using the fireball model,[3] and the hybrid formulation[4] of the exciton model.[5] They also demonstrated that a fit could be obtained by assuming the protons were evaporated isotropically (in the rest frame) from an excited moving source.

The velocity and temperature of the source, which they extracted from the fit assuming a simple exponential dependence of the cross section on particle energy in the moving frame, were one-half of the projectile velocity and 8.1 MeV.

Still another suggested explanation of the origin of the energetic light ions is that they are from evaporation from projectilelike fragments (PLF's) that have been excited during the collision. The evaporation-cascade calculations of Bertini *et al.*[6] have shown that this mechanism can explain the cross sections as a function of energy and angle of protons and deuterons produced when ^{56}Fe is bombarded with 192-MeV ^{12}C ions.[7]

Because the shape of inclusive spectra can be predicted by several quite different nuclear models, these data are not sufficient to definitively establish the reaction mechanism. For this reason there have been a variety of correlation experiments involving energetic light ions, with the greatest emphasis thus far placed on coincidences between energetic alpha particles and PLF's.[8–13] Similar studies have been performed recently with energetic neutrons[14,15] and protons.[16] Several interpretations have been given to explain the experimental results. References 8–11 concluded from the kinematical correlation of the emitted alpha particles with PLF's and from the narrowness and position of the maximum of the angular correlation of the alpha particles that the alpha particles were produced in a fast process at an early stage of the collision. In contrast, Bini *et al.*,[12] Young *et al.*,[13] and Schmitt *et al.*[16] reported that the coincident energetic light-ion spectra could be explained as evaporation from the PLF's and targetlike fragments (TLF's). Gavron *et al.*[14] found that to explain the fast neutrons from the bombardment of ^{93}Nb with 204-MeV ^{16}O they had to include, in addition to evaporation from PLF's and TLF's, a source of neutrons with a velocity of 70% of that of the projectile and a low temperature of 1.5 MeV.

Other studies indicate that some fraction of the energetic light particles is not associated with a PLF. Nonequilibrium light ions have been observed in coincidence with fusion residues or with γ rays characteristic with fusion residues by Westerberg *et al.*,[17] Geoffroy Young *et al.*,[18] and Gavron *et al.*[19] In Ref. 18 the neutron spectra were fitted by assuming some neutrons are evaporated from a moving source with a velocity of about one-half of the projectile velocity. This can be understood in terms of the incomplete fusion picture of Siwek-Wilczynska *et al.*[20] if, as shown in Ref. 18, the projectile is damped by some mechanism such as classical orbiting. Inamura *et al.*,[21] Zolnowski *et al.*,[22] and Yamada *et al.*[23] found evidence through particle-γ coincident measurements that energetic particles with both $Z=1$ and 2 are emitted in reactions which lead to fusion of the remaining PLF and target nucleus— a reaction which has been labeled as massive transfer.

Awes *et al.*[24] observed energetic $Z=1$ particles in coincidence with fission fragments following the bombardment of ^{238}U with 315-MeV ^{16}O. The proton spectra were explained by assuming the protons were isotropically emitted from a source moving with one-half the velocity of the projectile and with a temperature of 7.0 MeV.

It is also possible that some fast light ions are emitted unaccompanied by either fission fragments, fusion residues, or PLF's. Van Bibber *et al.*,[25] using a streamer chamber, observed a reaction with 35-MeV/nucleon ^{12}C on Ne that yielded nine charged-particle tracks. This may suggest that the reaction proceeds by disintegration of the projectile into a collection of light ions, some of which would have energies exceeding the average energy per nucleon of the projectile.

The experiments to date, when viewed collectively, indicate that there is more than one mechanism producing nonequilibrium light particles. Possibly because of a lack of information, there is not yet a consensus on what are the important reaction mechanisms, nor on what is the changing contribution of these processes as a function of projectile energy. Ideally, one would like to simultaneously measure all properties (kinetic energy, excitation energy, direction, mass, charge,...) of all particles and γ rays emitted in the collision. Obviously, in a real situation the experiment is limited by a finite number of detectors whose combination of type and location is limitless. This paper gives the results for one such measurement for the reaction of ^{12}C on ^{60}Ni. The experiment, which involved 16 detectors, observed a restricted angular distribution of energetic light ions in coincidence with (1) $Z=1,2$ particles, (2) PLF's, (3) γ-ray multiplicities, and (4) discrete γ rays. The discrete γ rays were used as signatures to identify the residual heavy fragments. The purposes of the experiment were to study the variation of light-ion spectra in coincidence with different gating particles and γ rays, and to study the variation depending on whether the light ions were protons or alpha particles. Measurements were performed for ^{12}C projectile energies of 136 and 194 MeV to determine if there

is beam energy dependence in the dominant reaction mechanism.

II. EXPERIMENTAL PROCEDURE

Beams of 136- and 194-MeV ^{12}C ions were obtained from the Oak Ridge Isochronous Cyclotron. The target was a 3.8-mg/cm^2 foil of ^{60}Ni. The target was mounted in a 15.2-cm-diameter scattering chamber with ports at 17°, 38°, −23°, and −49° that were covered with 0.05-mm-thick nickel foil. Light-ion telescopes composed of a Si transmission detector and a NaI(T1) detector with a 5.1-cm-deep crystal, were placed outside each port. The aluminum window of the NaI(Tl) crystal was 0.25 mm thick. For the 17° telescope the Si detector was 500 μm thick. For the other three angles the Si detectors were 1000 μm thick. The solid angles for the four light-ion telescopes ranged from 9.4 to 21.7 msr.

Inside the chamber there was a "heavy-ion" (HI) telescope at 17°, with an angular acceptance of ±4.4°, composed of two transmission Si detectors: one 75 μm thick and the other 750 μm thick. (The laboratory grazing angle for 194-MeV ^{12}C on ^{60}Ni is 9° and for 136 MeV it is 13°.) This telescope, which was used to observe PLF's and lower-energy $Z=1$ and 2 particles, was placed in front of the 17° light-ion telescope.

Two Ge(Li) γ-ray detectors were located in the plane of the particle detectors at +90° and −145°. A Pb filter was placed in front of each detector to reduce the contribution of low-energy γ rays and of x rays. Gamma-ray energies and absolute detector efficiencies were determined by means of a calibrated source placed at the target position. Above the scattering chamber were four 7.6×7.6 cm NaI(T1) detectors used for γ-ray multiplicity measurements.

Calibration of the E detector of the HI telescope was accomplished with the ^{12}C elastic scattering peak and with energies, as calculated from range-energy relations, deposited by lighter heavy ions that had just enough energy to penetrate the E detector. The light-ion NaI(T1) detectors were calibrated with recoil protons from a polyethylene target bombarded with the 136- and 194-MeV ^{12}C beams.

The data were stored event-by-event on magnetic tapes. An event was recorded if any one of the following coincidences occurred: (1) light-ion−light-ion, (2) light-ion−PLF, and (3) light-ion and γ-ray detected in either a Ge(Li) or NaI(T1) detector.

Proton and alpha spectra were observed as a function of angle and energy in coincidence with particles detected in the HI telescope at 17°. A ΔE versus E plot of events in this telescope showed groups corresponding to $Z=1$ to 7 particles. Free-form gates used to extract coincident spectra were drawn around each group of particles in this ΔE-E plot. The gates for the $Z=1$ and 2 particles were drawn to exclude those that had sufficient energy to reach the NaI(T1) crystal. That is, the upper energy limit for a gate for protons was 16 MeV, and for alpha particles it was 64 MeV.

When the coincidence was between a heavy ion and an energetic light ion both at 17°, the light ion would deposit some energy in the heavy-ion detector telescope, thereby distorting the ΔE-E spectrum. However, the separation between particle groups was sufficient to allow free-form gates to be drawn that included this broadening.

Coincidences between any two energetic light ions in any two of the four light-ion detectors were also studied. As above, gates were set around particle groups in the ΔE-E two-dimensional spectra.

Gamma rays observed in the Ge(Li) detectors in coincidence with the light ions were used to identify the residual nuclei. In many exit channels, the identification of a given isotope was based on the observation of one γ ray. This is because the yield was divided among so many channels that the γ rays of any given channel were weak, and few transitions among higher levels were observed. In these cases the certainty of identification is somewhat tenuous.

III. RESULTS

The proton energy spectra have very similar shapes in singles and when gated by various particles in the HI detector, although the slopes are somewhat steeper in the coincident spectra. There is no apparent structure except for the spectra observed in coincidence with carbon for a projectile energy of 136 MeV. For that case there is a large peak at $\theta_p=17°$ and $E_p\approx 17$ MeV that includes two groups with total kinetic energy $E_p+E_C\approx 120$ and 123 MeV. The latter is consistent with a single proton pickup to form $^{13}N^*$ (3.5 MeV) and subsequent decay by proton emission. The lower energy peak can be explained by the same process if the residual target nucleus is left in an excited state at about 3 MeV. In a two-dimensional plot between

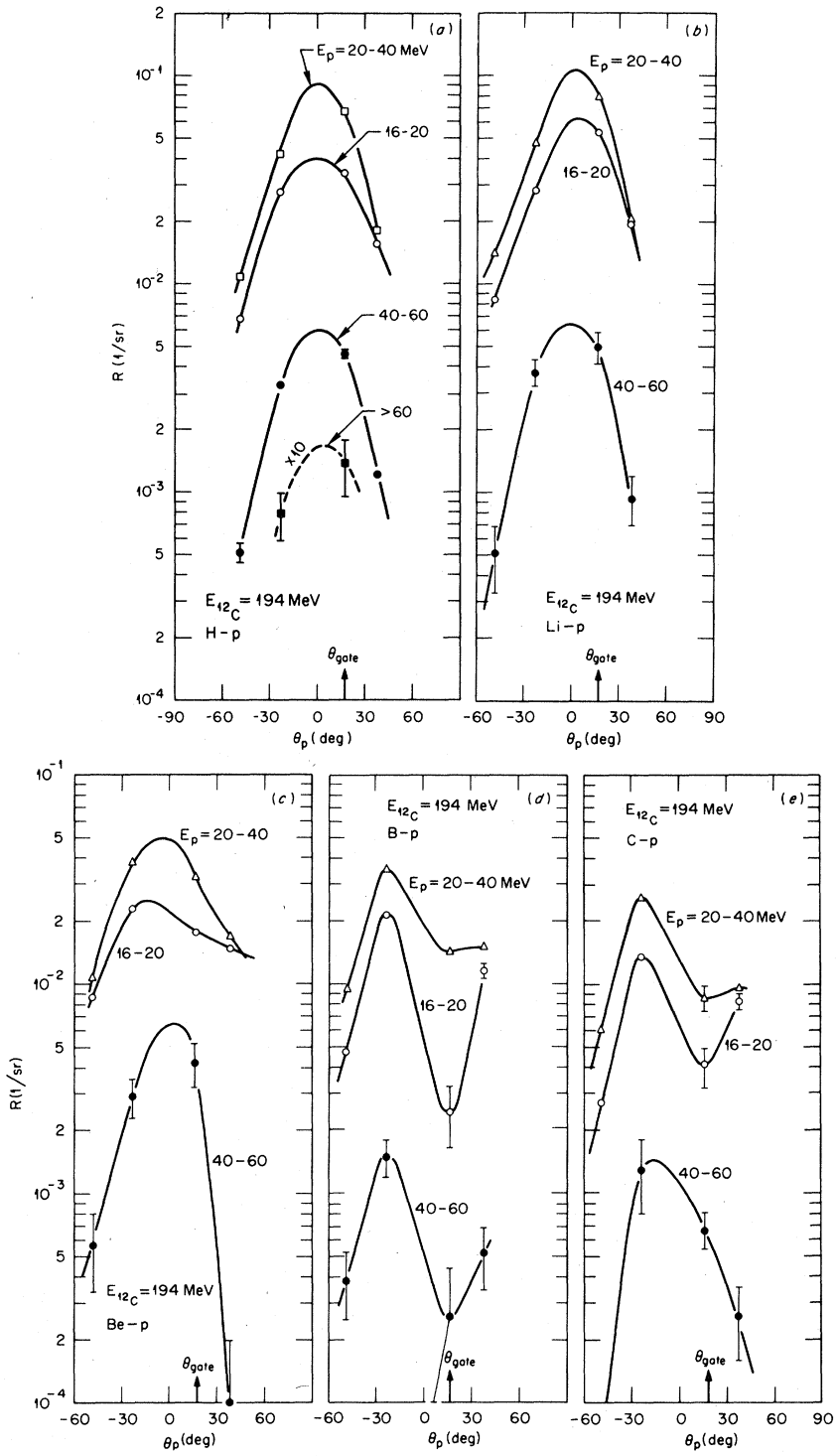

FIG. 1. Angular yields of the energetic protons in coincidence with (a) H, (b) Li, (c) Be, (d) B, and (e) C for a projectile energy of 194 MeV. The coincident protons are divided in the energy bins noted in the figures. The angle of the gating particles is 17°.

the energies of the coincident protons and C particles, about half of the protons with $E > 20$ MeV fall along a line for which $E_p + E_{12_C} \approx 123$ MeV. These could be explained by decay of higher excit-

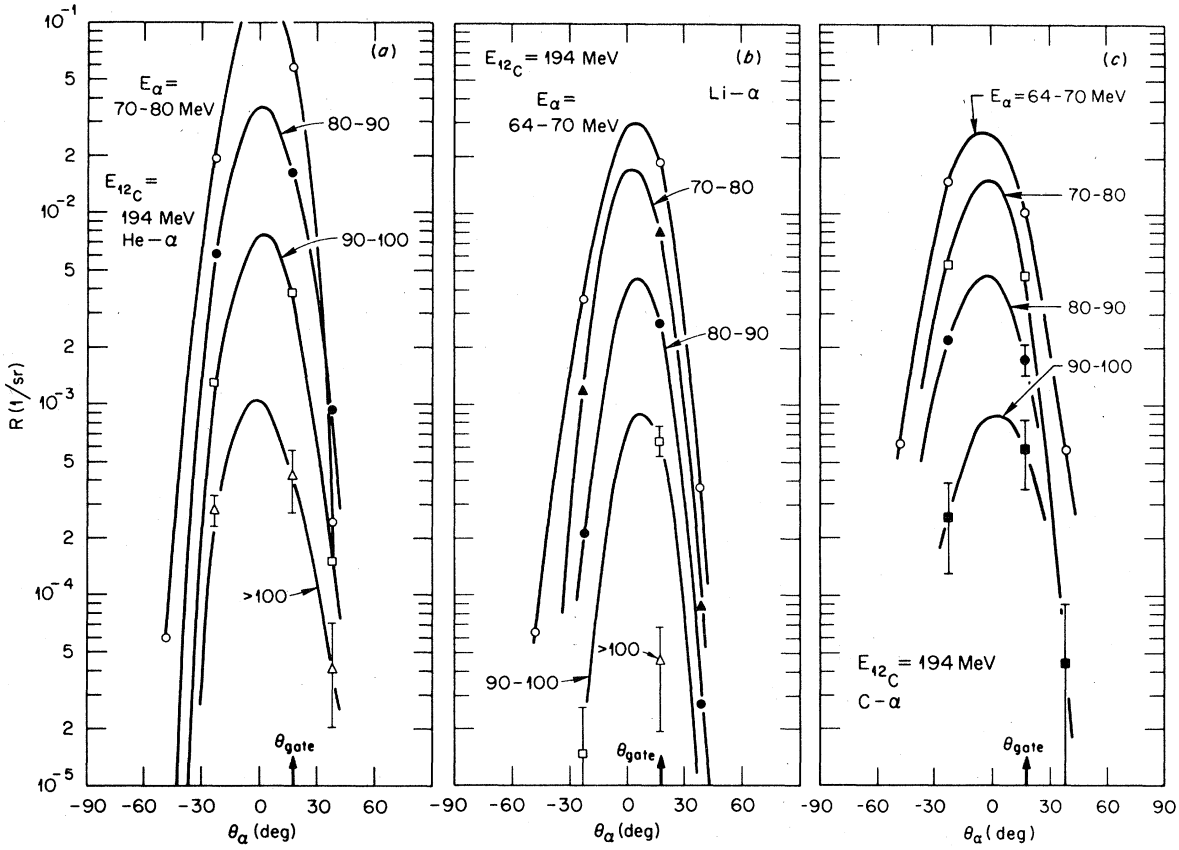

FIG. 2. Angular yields of the energetic alpha particles in coincidence with (a) He, (b) Li, and (c) C for a projectile energy of 194 MeV. The coincident alpha particles are divided in the energy bins noted in the figures. The angle of the gating particles is 17°.

ed states of ^{13}N following proton pickup. A similar band in the plot of E_p versus $E_{^{12}C}$ for a projectile energy of 194 MeV was not observed.

The energy spectra of alpha particles are also similar in the singles and coincident modes. No structure was seen in the spectra.

Representative angular yields of the energetic protons and alpha particles gated by different particles in the heavy-ion telescope are illustrated in Figs. 1–3. The gates include all particles with sufficient energy to penetrate the 75-μm ΔE detector of the heavy-ion telescope. In addition there is an upper energy limit for the gating $Z=1$ and 2 particles of 16 and 64 MeV, respectively. The ordinate in these plots is

$$R=\frac{N_c}{N_s\Delta\Omega}\ , \tag{1}$$

where N_c is the number of coincidences per μC of collected beam, N_s is the singles count of the gating particle per μC, and $\Delta\Omega$ is the solid angle of the light-ion detector. For the ^{12}C gate the elastic scattering peak was not included in the singles count.

To make a systematic comparison, the position of the centroid and the full width at half maximum (FWHM) have been determined for those distributions which have a simple peaked shape. These quantities are plotted in Figs. 4 and 5. The centroid position, with an uncertainty of about $\pm4°$ for protons and $\pm2°$ for alpha particles, generally peaks close to 0°. But there appear to be some small differences: The average centroid of the proton distribution occurs at more positive angles for the projectile energy of 136 MeV than for 194 MeV; for the alpha-particle angular distributions, the centroid position reaches a maximum positive angle for $Z=4$; and based on the 194-MeV data, the centroid angle generally increases with energy of the alpha particles. The FWHM is considerably

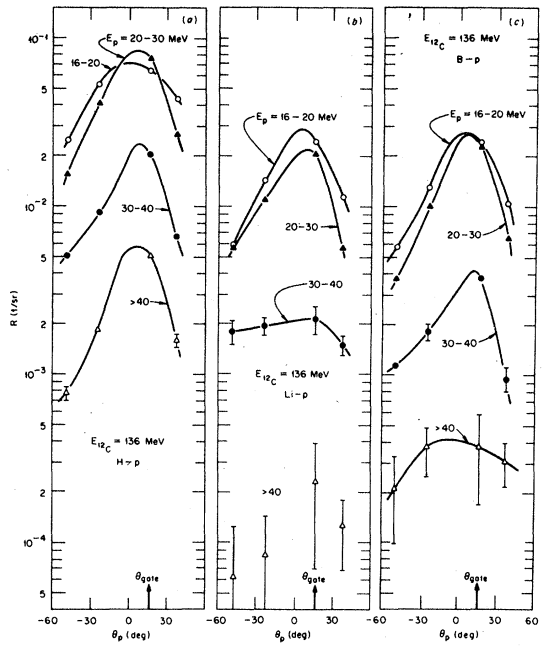

FIG. 3. Angular yields of the energetic protons in coincidence with (a) H, (b) Li, (c) B for a projectile energy of 136 MeV. The coincident protons are divided in the energy bins noted in the figures. The angle of the gating particles is 17°.

larger for protons ($\approx 50°$) than for alpha particles (30°).

For all gating heavy ions, the angular distribution of the alpha particles exhibits a single peak and is symmetric around the peak position. But the proton angular distributions cannot, in general, be so simply characterized. The most distinctive difference is for the 194-MeV data when gating on B, C, and N [see Figs. 1(d) and (e)]: this being a strong decrease in the coincident yield at about 17°. This minimum does not occur in the 136-MeV data. In other cases the proton angular distributions are not symmetric and are skewed to different sides; e.g., for the 194-MeV data, the distribution is skewed to positive angles when gating on Be [Fig. 1(c)], while in contrast, most of the 136-MeV results show skewness to negative angles. Another unusual case for $E_{12_C}=136$ MeV is observed when gating on Li, where the angular distribution for 30- to 40-MeV protons changes very slowly with angle [see Fig. 3(b)].

The multiplicity M of energetic protons and alpha particles that occur in coincidence with a gating heavy ion is related to the yield expressed in Eq. (1) by

$$M=\int R(\theta,\phi)\sin\theta\, d\theta\, d\phi\ . \tag{2}$$

However, since there were no measurements out of plane, the dependence of R on ϕ is unknown. To obtain at least the trend in M, we assumed that $R(\theta,\phi)$ varies as $1+\alpha\cos^2\phi$ with $\alpha=10$ and used results such as those given in Figs. 1–3 to integrate over θ. For distributions such as those illustrated in Figs. 1(d) and (e), it was assumed that the yield dropped away quickly beyond the four

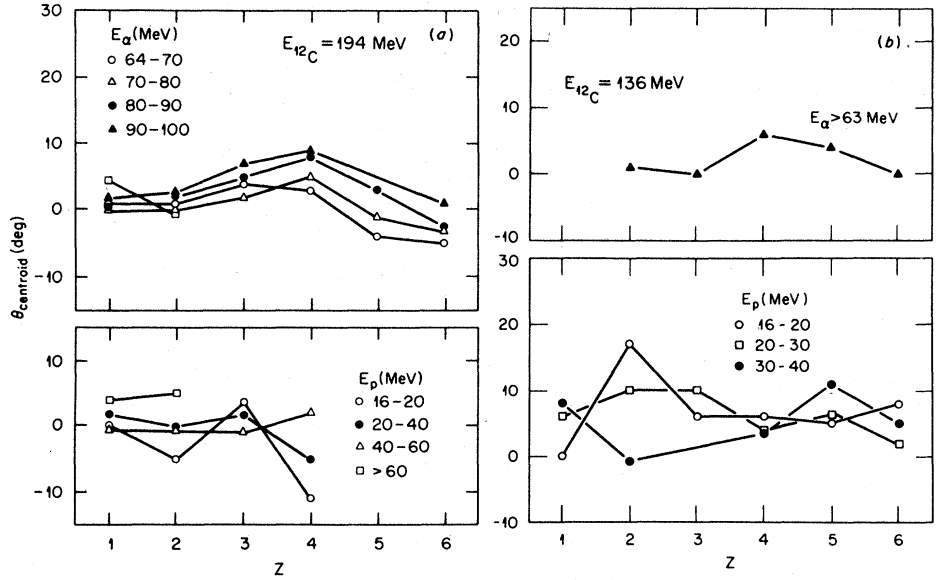

FIG. 4. The centroid of the angular distribution of the energetic protons and alpha particles when gating on particles with $Z=1$ to 6 for (a) $E_{12_C}=194$ MeV and (b) $E_{12_C}=136$ MeV.

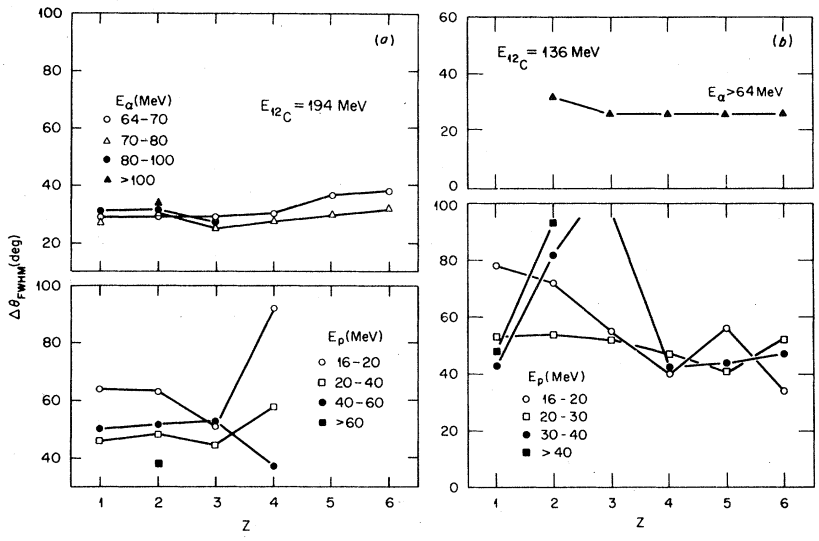

FIG. 5. The full width at half maximum of the angular distribution of the energetic protons and alpha particles when gating on particles with $Z=1$ to 6 for (a) $E_{^{12}C}=194$ MeV and (b) $E_{^{12}C}=136$ MeV.

angles measured. The resulting values of M are given in Figs. 6 and 7.

Three point angular distributions ($+38°$, $-23°$, and $-49°$) of energetic light ions were also obtained in coincidence with energetic light ions at 17°. Two-dimensional displays of the energies of the two coincident particles showed no obvious correlations. Within the uncertainties of fitting three points, the angular distributions had the same centroids and FWHM's as obtained when gating on the lower-energy protons and alpha particles. Multiplicities of energetic light ions occurring with other energetic light ions are given in Table I for $E_{^{12}C}=194$ MeV. They are generally comparable

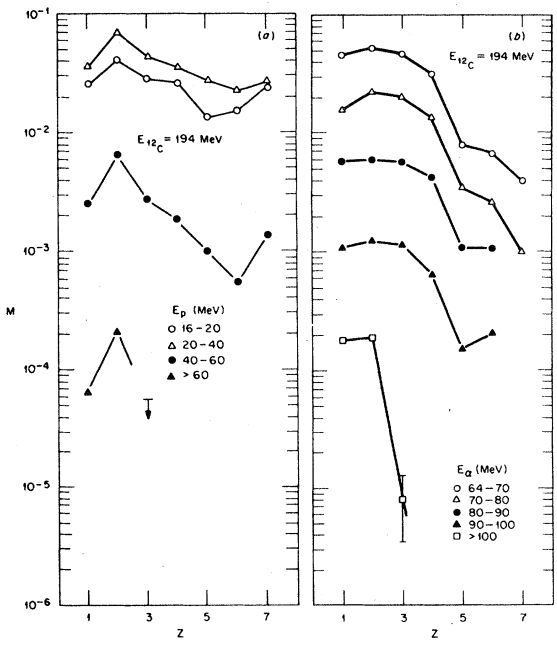

FIG. 6. The multiplicity of (a) protons and (b) alpha particles in the noted energy bins in coincidence with $Z=1$ to 7 particles. The projectile energy is 194 MeV.

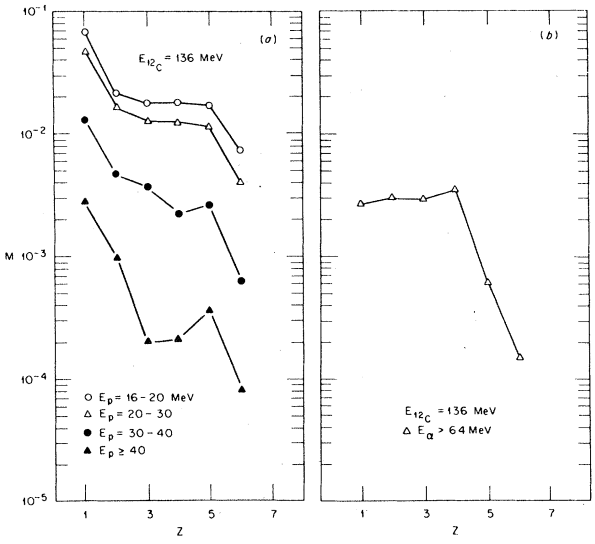

FIG. 7. The multiplicity of (a) protons and (b) alpha particles in the designated energy bins in coincidence with $Z=1$ to 6 particles detected at 17°. The projectile energy is 136 MeV.

TABLE I. Comparison of multiplicities of protons and alpha particles occurring in coincidence with protons and alpha particles detected at 17° for $E_{^{12}C}=194$ MeV.

light ion[a]	E (MeV)[a]	Multiplicity $E_p<16$ MeV[b]	$E_p>16$ MeV[b]	$E_\alpha<64$ MeV[b]	$E_\alpha>64$ MeV[b]
		$\times10^{-2}$	$\times10^{-2}$	$\times10^{-2}$	$\times10^{-2}$
p	16–20	2.5	2.6	4.0	1.1
	20–40	3.6	3.7	7.0	3.7
	40–40	0.25	0.38	0.65	0.38
α	64–70	4.6	3.3	5.2	12.6
	70–80	1.6	3.6	2.3	4.1
	80–90	0.58	0.082	0.60	0.50
	90–100	0.11		0.12	0.04

[a]Type and energy of particle observed in coincidence.
[b]Energy and type of gating particle.

(i.e., within a factor of 2) to multiplicities obtained when gating on the lower-energy light ion, as indicated in Table I.

The energies and intensities of γ rays detected in the Ge(Li) detector were determined for spectra in coincidence with protons and alpha particles. A sample spectrum is illustrated in Fig. 8. By forming the ratio of the observed particle-gamma coincidence yield $N_{p-\gamma}$ per μC of collected beam with the particle singles yield N_p per μC, one can introduce the quantity

$$q=\frac{N_{p-\gamma}}{N_p}\ . \tag{3}$$

which, when summed for all the ground-state γ-ray strength for a given nuclide, gives the fractional yield of that nuclide per particle recorded in the

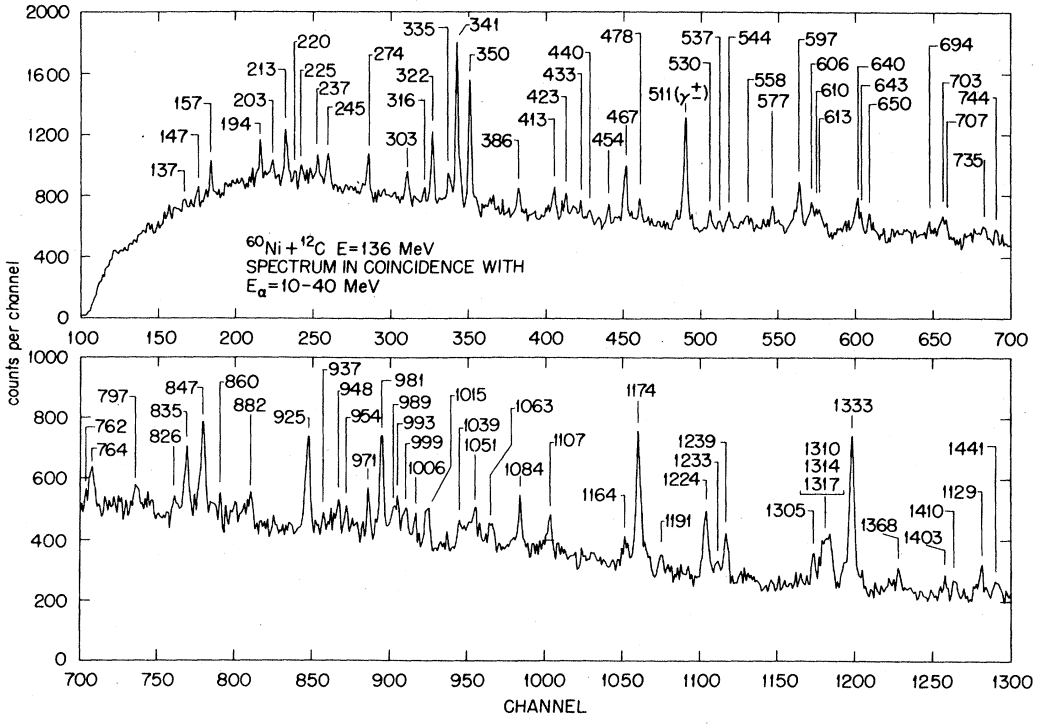

FIG. 8. Spectrum of γ rays in coincidence with alpha particles with energies of 10 to 40 MeV. The ^{12}C projectile energy is 136 MeV.

TABLE II. Residual targetlike fragments for ^{12}C with projectile energy of 136 MeV on ^{60}Ni.

Isotope	E_γ (keV)[a]	q (%)[b]			
		E_p (MeV)[c]		E_α (MeV)[c]	
		2.5–10	>16	10–40	>60
^{68}Ge	1016.5[d]	0.7(5)	1.3(5)	1.0(2)	<0.5
^{67}Ga	359.5	0.3(1)	1.2(3)	<0.3	<0.2
^{66}Ga	96.2	<0.4	<0.4	<0.3	<0.3
^{66}Zn	1039.4	1.4(5)	2.0(4)	1.1(2)	0.8(5)
^{65}Ga	190.6	1.0(2)[e]	1.7(3)[e]	≈0.1[e]	0.9(2)[e]
^{65}Zn	864.3, 1047.3	3.1(6)	3.5(7)	1.0(2)	1.8(6)
^{64}Zn	991.5	3.7(4)	5.5(5)	1.2(3)	4.9(3)
^{64}Cu	159.3	0.3(1)	<0.3	<0.1	0.2(1)
^{63}Zn	192.9, 550.2, 1064.1	1.3(4)[e]	3.6(6)[e]	2.7(7)[e]	5.0(5)[e]
^{63}Cu	962.1, 1327.0	1.9(3)	1.6(4)	0.8(3)	1.3(3)
^{62}Zn	953.9	1.3(3)	1.6(4)	0.6(2)	1.8(3)
^{62}Cu	243.4, 349.3, 385.3[f]	3.7(4)	4.0(4)	3.8(3)	7.3(4)
^{62}Ni	1172.9[g]	?	?	?	?
^{61}Cu	970.0, 1310.5	4.1(5)	2.6(5)	3.0(5)	5.2(5)
^{61}Ni	947.6, 1015.0[e,h]	1.8(4)	2.1(4)	1.0(2)	1.8(3)
^{60}Ni	1332.5	5.9(3)	4.6(4)	8.4(4)	7.7(4)
^{59}Ni	339.3, 878.0, 1189.1, 1337.9[i]	2.1(3)	2.4(3)	4.9(3)	3.1(3)
^{59}Co	1190.6, 1459.6	2.0(10)	2.9(4)	2.5(5)	2.0(4)
^{58}Ni	1454.4	≤0.5	≤0.8	1.8(4)	0.7(4)
^{58}Co	58.5,[j] 111.7, 321.0, 365.7, 432.7, 1050.0	1.9(6)	1.7(6)	4.2(7)	3.3(7)
^{57}Co	1223.7, 1689.4	2.5(4)	<0.9	4.7(2)	1.8(3)
^{57}Fe	1061.6	0.7(3)	0.8(4)	0.6(3)	1.2(4)
^{56}Co	576.5	0.7(2)	0.5(2)	0.9(2)	<0.3
^{56}Fe	846.8	1.8(3)	1.6(5)	2.9(2)	0.8(3)
^{56}Mn	212.0, 335.5, 454.3	1.1(3)	1.2(4)	1.4(3)	0.6(3)
^{55}Fe	931.4,[k] 1316.8,[k] 1408.5[k]	≤4.0	≤3.0	≤3.0	≤2.0
^{55}Mn	126.0	<1.0	0.4(2)	<0.2	<0.1
^{55}Cr	242.1, 517.8, 565.9, 880.7	<1.7	<0.6	<0.6	<1.1
^{54}Fe	1408.2[l]	0.8(4)	1.2(4)	0.8(3)	1.0(4)
^{54}Mn	156.3	0.3(2)[e]	0.3(2)[e]	0.6(1)[e]	0.4(2)[e]
^{54}Cr	834.9	1.3(2)	1.3(3)	1.5(2)	0.8(2)
^{53}Cr	1006, 1290	0.8(5)	0.6(4)	1.0(4)	0.5(2)

[a] γ rays assumed to contain all the strength to the ground state.
[b] Yield in percent of residual fragment per detected energetic proton or α particle as indicated. The errors are given by the numbers in parentheses.
[c] Energy of gating particles.
[d] Corrected for contribution from 1015.0-keV γ ray in ^{61}Ni.
[e] 90° detector value.
[f] Corrected for contribution from 385.3-keV γ ray in ^{55}Fe.
[g] Not resolved from 1173.2-keV γ ray in ^{60}Ni.
[h] Partially due to ^{68}Ge. Based on the ^{61}Ni decay scheme, we adopt $I(1015\gamma)=0.039I(947.6\gamma)$.
[i] Not resolved from strong 1332-keV γ ray in ^{60}Ni. Based on the ^{59}Ni decay scheme, we adopt $I(1337.9\gamma)=0.429I(998.4\gamma)$.
[j] Too low in energy to be seen here. Based on the ^{58}Co decay scheme, we adopt $I(58.5\gamma)=0.89I(111.7\gamma)$.
[k] Upper limit only for 931.4-keV γ ray. The 1316.8- and 1408.5-keV γ rays are seen but are not due entirely to ^{55}Fe. From the decay scheme, $I(1316.8\gamma)\leq 13.7I(931.4\gamma)$ and $I(1408.5\gamma)\leq 0.71I(931.4\gamma)$.
[l] Corrected for contribution from 1408.5-keV γ ray in ^{55}Fe.

gating detector. In calculating $N_{p-\gamma}$ it was necessary to integrate over all angles for γ-ray emission. For this, it was assumed the γ rays are emitted isotropically with a value per unit solid angle taken as the average value of the yield in the two Ge detectors. It was assumed that for even-even nuclei all the intensity feeding the ground state was contained in the transition from the first 2^+ level to the ground state. Intensities of transitions between higher levels were checked where possible to confirm the nuclide identification and to obtain an estimate of the relative feeding of higher-spin levels. For odd-A and odd-odd nuclei, it was necessary to make use of other (HI, $x\gamma$) data to deduce the probable heavy-ion decay schemes. Since in these decays the γ-ray strength to the ground state is, in general, spread over many transitions, the extracted absolute yields for these nuclei are less reliable. Because of the low number of coincidence counts, the gating particles were divided into only two energy bins, one covering primarily the evaporation region, and the other the nonequilibrium particles.

The distribution of residual nuclei as extracted from the γ-ray data is given in Table II. The nuclei and identifying γ rays are given in the first two columns. The γ rays shown are those assumed to carry all the intensity to the ground state. The deduced q values for the gates $E_p = 2.5-10$ MeV, $E_p > 16$ MeV, $E_\alpha = 10-40$ MeV, and $E_\alpha > 60$ MeV are given in columns 3–6. There are many channels with the consequence that no channel is very

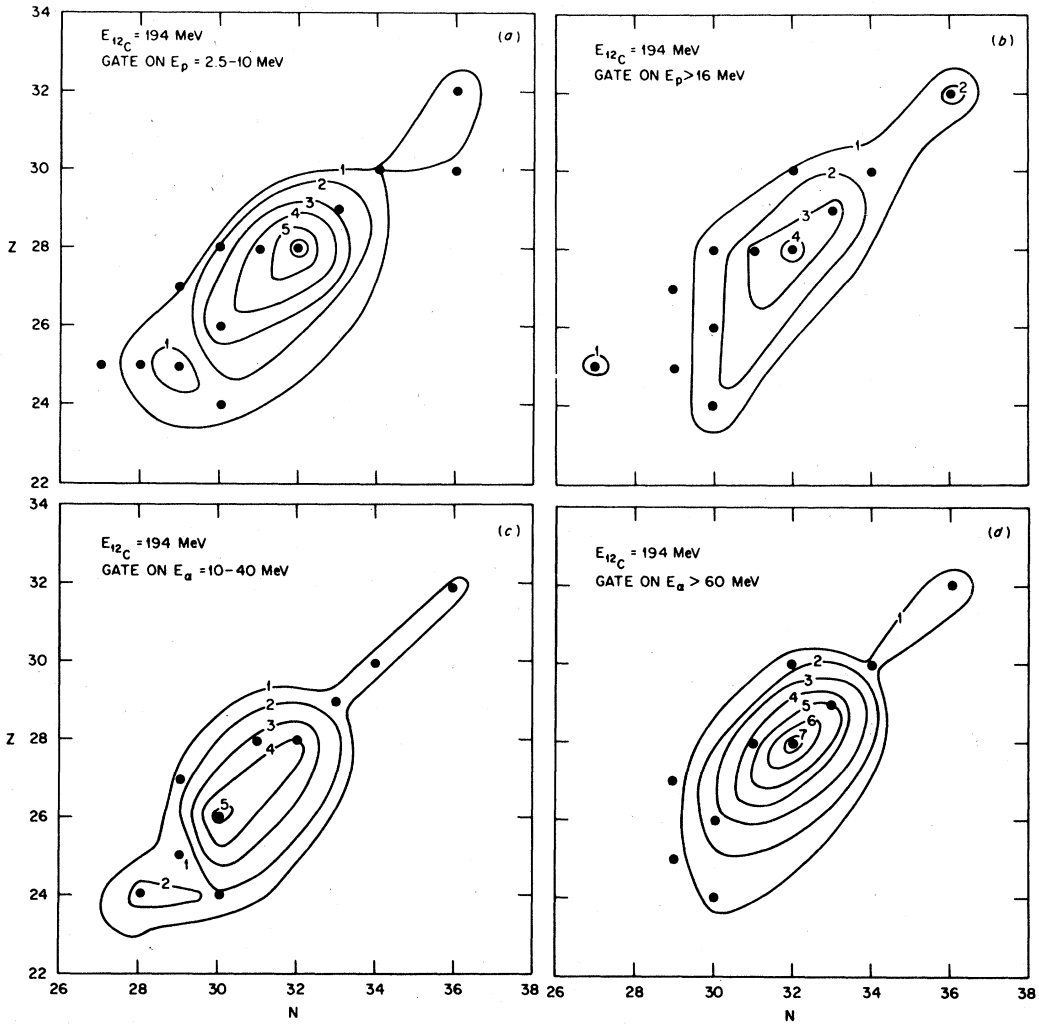

FIG. 9. Distribution of residual nuclei for a projectile energy of 194 MeV in coincidence with (a) 2.5- to 10-MeV protons, (b) > 16-MeV protons, (c) 10- to 40-MeV alpha particles, and (d) > 60-MeV alpha particles. The contour lines correspond to percent of all coincident residual nuclei. The locations of the measured points on which these contour lines are based are indicated by solid circles.

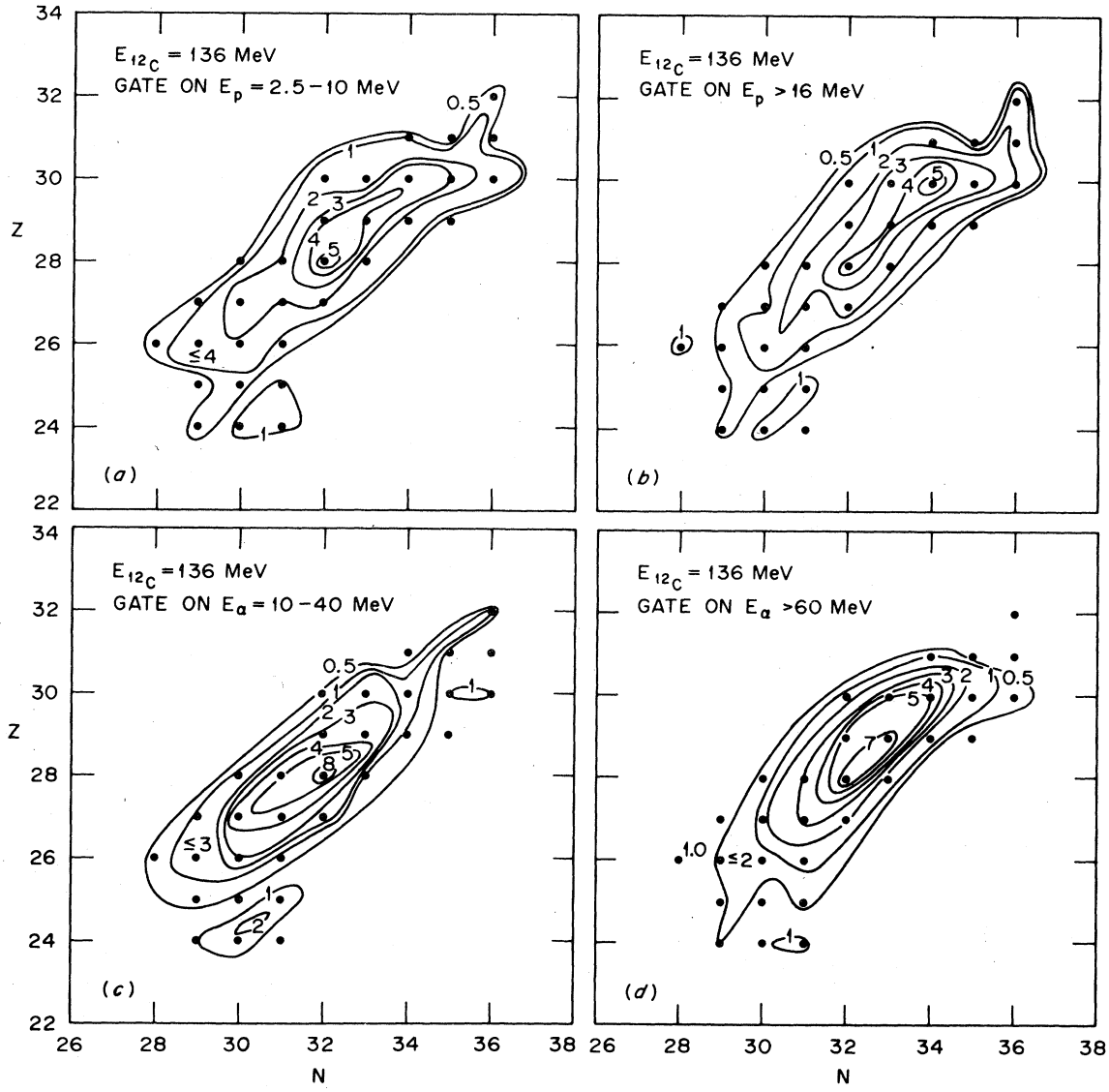

FIG. 10. Distribution of residual nuclei for a projectile energy of 136 MeV in coincidence with (a) 2.5- to 10-MeV protons, (b) > 16-MeV protons, (c) 10- to 40-MeV alpha particles, and (d) > 60-MeV alpha particles. The contour lines correspond to percent of all coincident residual nuclei. The locations of the measured points on which these contour lines are based are indicated by solid circles.

strong. The strongest channel observed is 8.4% for the production of ^{60}Ni in the $E_\alpha = 10$- to 40-MeV gate for a ^{12}C projectile energy of 136 MeV.

Plots of production of the residual nuclei versus N and Z, as generated from the values given in Table II, are illustrated in Figs. 9 and 10. Ideally, the sum of the production of all nuclei as extracted from the contour lines should be 100%. In actuality, for the 136-MeV data the sums as obtained from Figs. 10(a)—(d) are, respectively, 55%, 57%, 58%, and 56%. The uncertainties due only to counting statistics and efficiency corrections are 5—10%.

One explanation for these low values could be associated with the problem mentioned above that, especially for odd-A and odd-odd nuclei, not all the cascades feeding the ground state may have been observed. The sensitivity for detecting a single γ ray, in terms of the q value, ranges from $q \approx 0.2\%$ at $E_\gamma = 200$ keV to $q \approx 0.8\%$ at $E = 1300$ keV. It should also be noted that the ratio $q(90°)/q(-145°)$ for a given γ ray ranges from 1 to 2 with most values in the upper half of this range. Thus, angular distribution effects are signi-

ficant. Unfortunately, the relatively low peak counts did not allow a quantitative study of these effects as a function of energy and type of gating particle.

No general conclusion could be drawn regarding the feeding of high-spin states. However, a few specific examples can be given. In the case of ^{60}Ni with a ^{12}C projectile energy of 136 MeV, values of $q(4^+\rightarrow 2^+)/q(2^+\rightarrow 0^+)=0.74\pm0.08$, $q(6^+\rightarrow 4^+)/q(2^+\rightarrow 0^+)=0.35\pm0.05$, and $q(7\rightarrow 6^+)/q(2^+\rightarrow 0^+)=0.21\pm0.07$ were obtained. For ^{56}Fe, $q(4^+\rightarrow 2^+)/q(2^+\rightarrow 0^+)=0.75\pm0.13$.

In the 194-MeV data, the peak of the contour "mountain" is at ^{60}Ni for gates on both high- and low-energy protons, and on the high-energy alpha particles. Thus, the average total of nucleons emitted through all processes is approximately equal to that of the projectile. The contour plot obtained through coincidence with lower-energy alpha particles peaks at $\approx^{56}Fe$. Possibly, additional particles are emitted since there is more energy available for other processes when the gating particle has less energy.

In the 136-MeV data the peak of the residual nucleus distribution (Fig. 10) is at ^{60}Ni for low-energy protons and alpha particles. For high-energy protons the distributions are double peaked with maxima at ^{64}Zn ($q=5.5\pm0.5$) and ^{60}Ni ($q=4.6\pm0.4$); for high-energy alpha particles the contour plot may also be double peaked with maxima at ^{62}Cu ($q=7.3\pm0.4$) and ^{60}Ni ($q=7.7\pm0.4$).

The number of the four NaI detectors observing

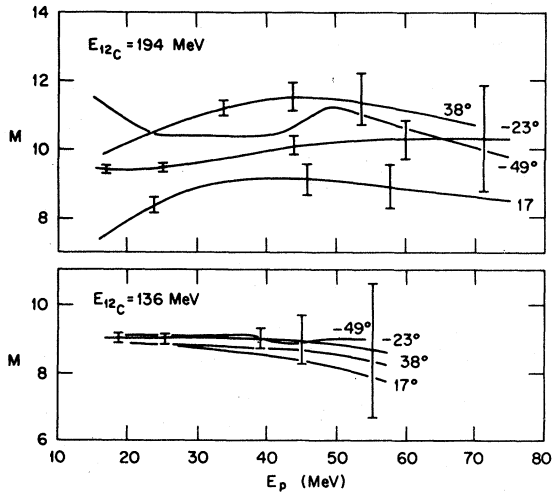

FIG. 11. Smooth curves drawn through experimental multiplicities of γ rays in coincidence with protons of energies given on the abcissa. The angle denotes that of the proton detector. Representative error bars are illustrated.

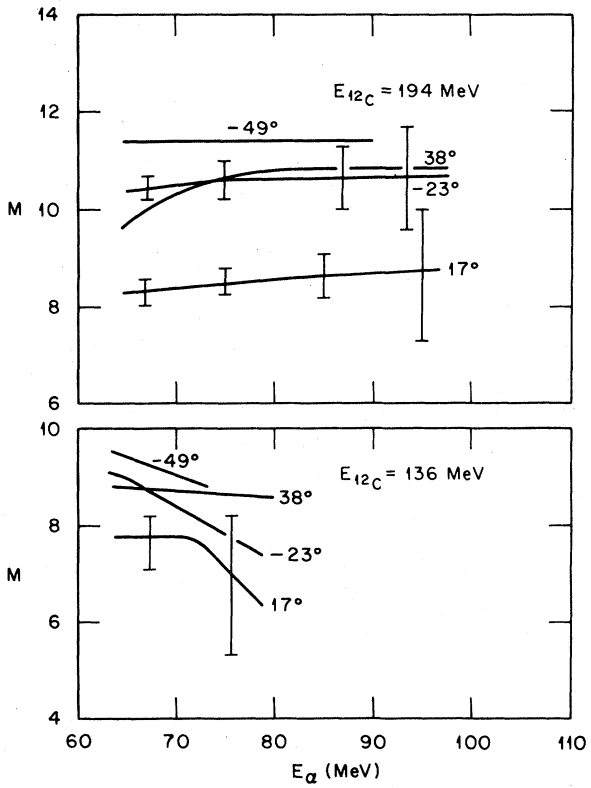

FIG. 12. Smooth curves drawn through experimental multiplicities of γ rays in coincidence with alpha particles of energies given on the abcissa. The angle denotes that of the alpha detector. Representative error bars are illustrated.

γ rays simultaneously in coincidence with the energetic light ions were used to obtain the zero- to four-fold light-ion spectra. From these spectra the multiplicities of γ rays were extracted by means of the technique discussed by Hagemann *et al.*[26] Smooth curves visually fitted to these deduced multiplicities are plotted in Figs. 11 and 12 as a function of the energy of the gating particle. The curves are plotted for each of the four light ion detectors.

IV. DISCUSSION

The ultimate goal is to understand the reaction mechanisms leading to emission of nonequilibrium light ions from heavy-ion induced reactions. These light ions represent a majority of those whose energy per nucleon exceeds that of the projectile. In this section we examine several features of the present experimental results and comment on possible implications of these features. In the next section, Monte Carlo calculations are used to provide some quantitative comparisons with experiment. The discussion here is divided into three

parts which compare the results for (i) the two projectile energies, 136 and 194 MeV, (ii) emission of energetic protons and alpha particles, and (iii) different energies of the emitted light ions.

(i) We find that the single-peaked angular distributions of the protons and of the alpha particles observed in coincidence with PLF's are generally comparable at the two projectile energies, except that the centroid of the proton angular distributions occurs at a somewhat more positive angle for $E_{^{12}C}=136$ MeV than for 194 MeV. This can be seen from plots of the centroid of the peaks and their FWHM as given in Figs. 4 and 5. However, there is one striking difference between the two projectile energies: For some particle energies the angular distribution of the protons emitted from 194-MeV projectile bombardment shows a strong decrease at 17° for gating particles with $Z=5-7$. That is, these PLF's have a smaller likelihood of being emitted in the same direction as the energetic proton. Another difference for the proton data observed between the two projectile energies is that for the 136-MeV projectile energy the angular distributions appear consistently skewed toward negative angles (compare Figs. 1 and 3). These effects suggest that in addition to the dominant reaction process giving rise to the strongly peaked, symmetric angular distribution, there is some other weaker process. More complete angular distributions would be required to explore this feature.

The multiplicities of γ rays in coincidence with energetic protons and alpha particles are somewhat larger for 194-MeV ^{12}C data than for 136 MeV (Figs. 11 and 12). This appears consistent with the predominant reaction mechanism being the same at both energies, since the higher-energy projectiles bring in more angular momentum on average. A comparison of Figs. 9 and 10 shows that for all gates, as the bombarding energy is lowered from 194 to 136 MeV, the centroids of the contour maps of the residual nuclei shift to higher mass along the $N=Z+4$ line even though for some contours the main peak remains at ^{60}Ni. This, too, seems resonable if the principal reaction mechanism is the same at both energies as the additional energy provided by the higher-energy projectiles would cause more particles to be emitted.

A striking difference is observed in the multiplicity plots of the energetic protons for the two projectile energies [see Figs. 6(a) and 7(a)]. Namely, the ratio of multiplicity of protons extracted when gating on $Z=1$ and $Z=2$ particles is ≈ 0.5 for the 194-MeV projectiles, whereas it is ≈ 3 for 136-MeV projectiles. We have no explanation to offer for this phenomenon.

(ii) The angular distributions for the alpha particles are substantially narrower than for the protons (see Fig. 5). Furthermore, the width of the angular distributions for the alpha particles (see Fig. 5) is remarkably independent of the Z of the gating PLF, the energy of the alpha particles, and of the projectile energy. Although there are some special cases for the proton angular distributions, the widths given in Fig. 5 taken as a group do not show any systematic trends with Z of the gating particle, with the energy of the proton, or with projectile energy. The behavior of these angular distribution widths is not consistent with calculations for complete fusion (CF) or for the deep, inelastic collision process (DIC) (see Sec. V). The absence of variation in the widths of the angular distributions with energy of the emitted particle and Z of the gating particle; the small variation observed in the peak position, and the peak position of approximately 0° are reasonable features if a large part of the energetic light-ion emission takes place early in the collision process and the gating PLF's retain little memory of emission of the light ions.

The charged-particle multiplicity plots as shown in Figs. 6 and 7 are different for the protons and alpha particles. Most noticeable is the sudden drop between $Z=4$ and 5 in the multiplicity of alpha particles. A likely explanation is that many of the alpha particles are emitted from breakup of the ^{12}C projectile. But to be consistent with the features discussed in the previous paragraph, the breakup must take place early in the collision process. A corresponding decrease between $Z=5$ and 6 in the proton multiplicity is not observed with $E_{^{12}C}=194$ MeV. This indicates that few fast protons come from the simple process of C breaking up into $B+p$ without further breakup of the B fragment. For the 136-MeV data there is a strong drop between $Z=5$ and 6. However, the uncertainty of the $Z=6$ point is large because of the low-energy tail from the strong elastic peak in the gating spectrum. The observation of alpha particles in coincidence with $Z\geq 5$ particles and protons with $Z\geq 6$ particles shows that at least some energetic $Z=1,2$ particles do not come from the projectile in a one-step process.

(iii) Figures 6(a), 6(b), and 7(a) all show that for the most energetic protons and alpha particles, the multiplicities obtained with the higher Z gates are relatively smaller than for $Z=1,2$ gates as com-

pared to the lower-energy light ions. The implication is that there is a component of the very energetic light-ion spectra that is not associated with a process in which a PLF remains, i.e., not from a process such as DIC.

The multiplicity of γ rays in coincidence with energetic protons and alpha particles is relatively insensitive to the particle energy (see Figs. 11 and 12). If the average angular momentum associated with each γ ray is between 1.5 and 2, the spin of the state from which the γ-ray cascade occurs would be $\approx 15-20\hbar$. This is well below the limit for the maximum angular momentum of $\approx 50\hbar$, where for this mass region the fission barrier vanishes.[27] It is comparable to what is expected for a fusion reaction[28] where the maximum angular momentum is $\approx 25\hbar$ in the entrance channel. It has been suggested that for heavier targets massive transfer has associated with it the emission of energetic light ions and should result in residual nuclei with higher average angular momenta[21-23] than obtained through a total fusion process. Our results do not support the idea that the average angular momentum reached in the residual nucleus is higher when associated with high-energy light ions.

An interesting result discussed in Sec. III was that the multiplicity of an energetic light ion obtained for $E_{^{12}C}=194$ MeV occurring in coincidence with light ions was comparable whether the gating energy was low or high (see Table I). Furthermore, energy-energy two-dimensional spectra of the two coincident $Z=1,2$ particles showed no correlation. The implication is that the fast light ions are emitted in an early stage of the reaction and other light ions are emitted in subsequent reaction stages which have no memory of the early stage.

V. COMPARISONS TO MONTE CARLO CALCULATIONS

Monte Carlo calculations were performed for the complete fusion and deep inelastic collision process for the $^{12}C+^{60}Ni$ system by means of the computer program LILITA.[29] For CF the values of the critical angular momentum l_{cr} were determined with the sharp cutoff approximation, and the fusion cross section σ_{fus} was calculated with the critical distance model.[30] With the assumption of the critical potential $V_{cr}=0$, the fusion cross section is given by

$$\sigma_{fus}=\pi R_{cr}^{2}\,, \tag{4}$$

where

$$R_{cr}=r_{cr}(A_P^{1/3}+A_T^{1/3})\,. \tag{5}$$

A value of $r_{cr}=1.0$ fm was chosen since it gives a good fit to the measured fusion cross section resulting from bombardment of ^{63}Cu with 167-MeV ^{20}Ne.[31] The calculational method for the DIC case was similar to that described in Ref. 32. The most probable Q value (Q_M) is given by

$$Q_M=E_{Kc.m.}-E_{c.m.}\,, \tag{6}$$

where the total kinetic energy of the fragments is

$$E_{Kc.m.}=Z_PZ_Te^2/d+\hbar^2l_f(l_f+1)/2\mu d^2\,, \tag{7}$$

and $E_{c.m.}$ is the energy of the projectile in the center of mass. The quantity d is the separation distance of the fragment at scission, μ is the reduced mass, and l_f is the relative orbital angular momentum. The values of d and l_f used in the DIC calculations are deduced from the analysis[30] of the $^{20}Ne+^{63}Cu$ reaction; they have been scaled only by the Z_PZ_T and $(A_P^{1/3}+A_T^{1/3})$ factors. Also, a spread in Q_M has been included and was taken as $\Delta Q/Q_M=10\%$.[32] The equilibrium assumption is used to determine the amount of excitation energy carried away by the TLF's and PLF's, i.e., the average excitation energy of the fragments is determined by their mass ratio.

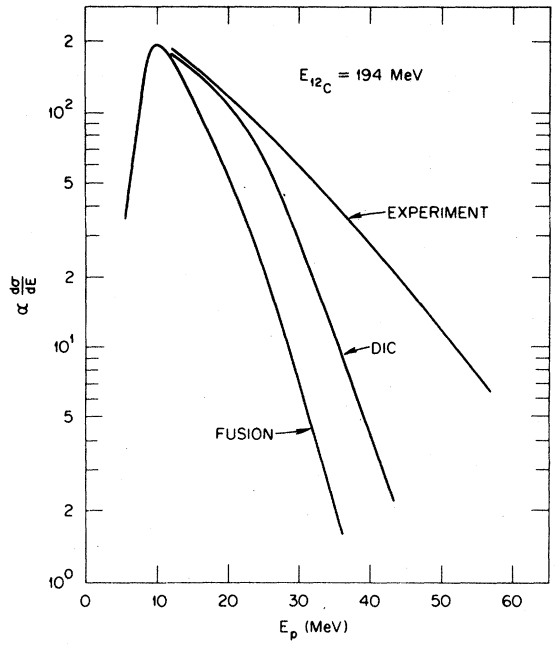

FIG. 13. Inclusive proton spectra at 17° for 194-MeV ^{12}C bombardment of ^{60}Ni. The "experiment" line is a smooth fit to the experimental data. The other two curves are calculated for a fusion reaction and for a deep inelastic collision process. They are normalized to the same value at $E_p\approx 10$ MeV.

Results of these calculations for the inclusive proton spectra for 194-MeV ^{12}C on ^{60}Ni are illustrated in Fig. 13. Also shown is the experimental inclusive spectrum. The curves are normalized to the same yield at $E_p \approx 10$ MeV. This comparison shows that neither CF nor DIC can account for the majority of fast protons. Calculations for CF and DIC also fail to explain the FWHM of the experimental angular distributions. For example, for the angular distribution of 27-MeV protons, the calculated FWHM's are 96° and 32°, respectively, for CF and DIC. The experimental width is 50°. For 40-MeV alpha particles, the corresponding FWHM's are 52° and 48°, whereas the experimental widths for $E_\alpha > 64$ MeV is 30°. Furthermore, the calculated FWHM's are a strong function of the energy of the light ions, whereas experimentally this is not the case (see Fig. 5). Thus, according to these calculations many of these fast particles are not associated primarily with evaporation from a completely fused system or with DIC.

In addition, the LILITA calculations predict the distribution of the residual nuclei and the γ-ray multiplicity. Comparison of the experimental and calculated γ-ray multiplicities is given in Table III. Comparisons of the distributions of the residual nuclei as a function of Z and A are shown in Fig. 14 for the two bombarding energies of 136 and 194 MeV. The comparisons between the experimental distributions resulting from coincidences with low-energy alpha particles and the calculated ones for CF, shown in Figs. 14(b) and (d), are particularly useful, since the good agreement, especially at 136 MeV, indicates that the observed distribution is due to CF. Also given in Figs. 14(b) and (d) are the experimental yields of residual nuclei resulting from coincidences with high-energy alpha particles. For these distributions, there is a clear shift of nearly two units in Z relative to the low-energy alpha-particle results and CF calculations. This indicates that the large energy release due to the emission of the fast alpha particles reduces considerably the excitation energy of the system and, therefore, the amount of evaporation. In this regard, it is illustrative to comment on the Z and A distributions predicted by the Monte Carlo calculations for the case of DIC (solid histograms in Fig. 14). As can be seen in Fig. 13, the DIC process is capable of producing higher-energy light particles than the CF case and, therefore, could account for some of the features of the energetic light-particle emission. However, the Monte Carlo calculations predict centroids of the Z and A distributions for DIC that are too low as compared to experiment. This suggests that most of the light-particle emission is due to processes other than DIC. This statement is also consistent with the low multiplicities of protons and alpha particles observed in coincidences with PLF's (see Fig. 6). The low values of the centroids of the Z and A distributions predicted for DIC are due to the large negative Q values and the two-body-like nature of the DIC process as well as the equilibrium assumption that gives more excitation energy to the TLF's. Because of this large excitation energy for the TLF's, evaporation is an important process.

TABLE III. Comparison of the experimental and calculated γ-ray multiplicities. The CF and DIC values were calculated with the program LILITA.

Type	$\langle M_\gamma \rangle$
194-MeV $^{12}C+^{60}Ni$	
Experiment	10 ±1
CF	10.0
DIC	8.3
136-MeV $^{12}C+^{60}Ni$	
Experiment	9 ±1
CF	10.2
DIC	7.9

The yields of residual nuclei resulting from coincidences with protons are shown in Figs. 14(a) and (c). The experimental distributions are essentially the same whether the gate is on low- or high-energy protons. This result is different than that found for alpha-particle emission. In addition, one sees that the centroids of the Z and A distributions predicted by both the CF and DIC calculations are too low compared to experimental results obtained when gating on protons. This indicates that even protons with energies between 2.5 to 10 MeV are primarily due to a process other than CF or DIC.

The agreement between the experimental distribution of residual nuclei as obtained when gating on the higher-energy light ions and those calculated for CF, although not good, is substantially better than for those calculated for DIC. Also, the CF predictions for γ-ray multiplicity are somewhat more similar to the experimental results than those of DIC (see Table III). These comparisons indicate that the predominant reaction mechanism is more akin to evaporation from a fused system than to a process where the PLF stays intact.

A picture suggested by the comparison to the

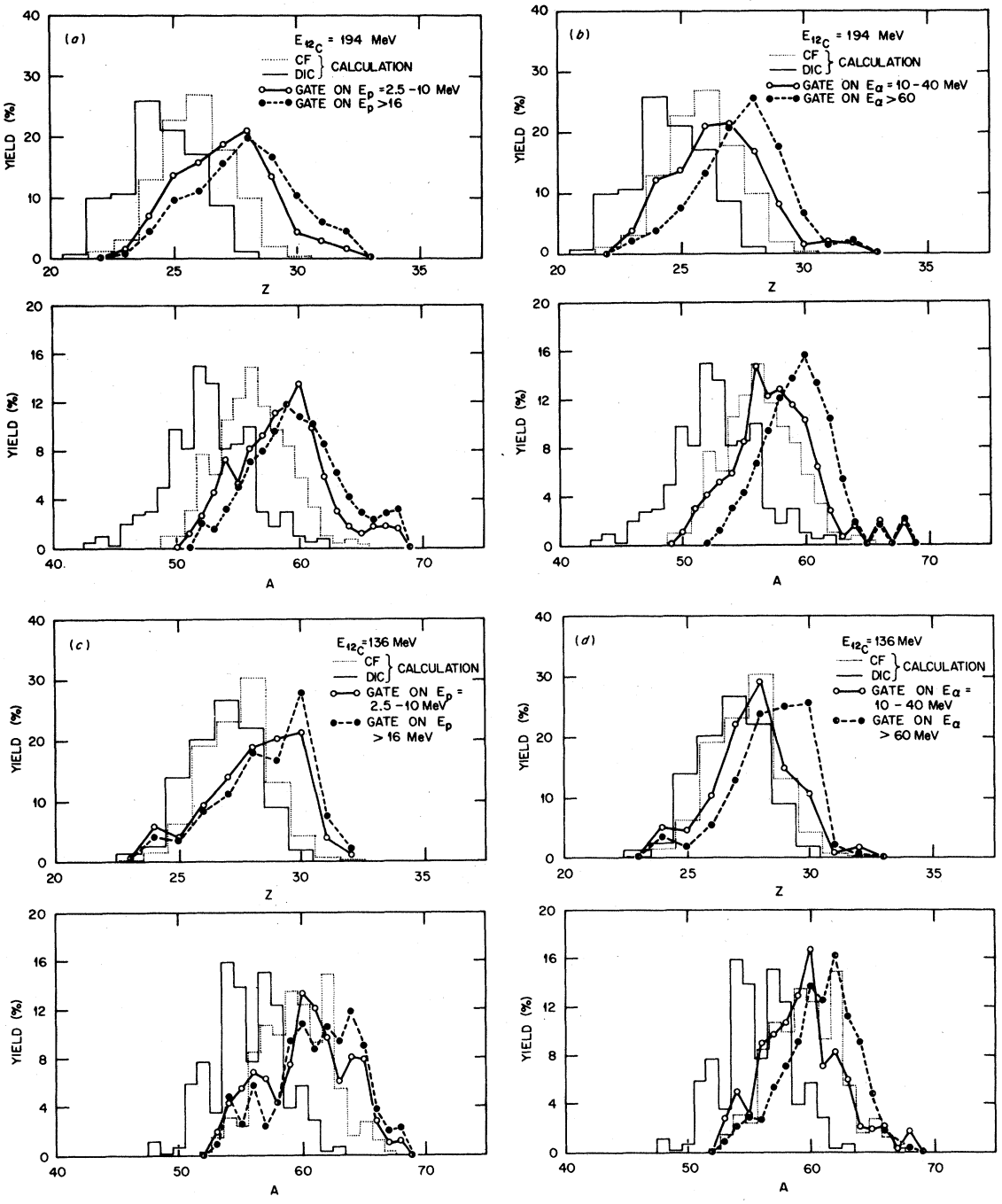

FIG. 14. The distribution of the residual nuclei as a function of Z and A. The experimental values denoted by the open and closed circles are obtained from Figs. 9 and 10. The histograms are calculated with the program LILITA for CF and DIC. The projectile energy and type of emitted particle for each pair of figures are, respectively: (a) 194 MeV, protons, (b) 194 MeV, alpha particles, (c) 136 MeV, protons, and (d) 136 MeV, alpha particles.

Monte Carlo calculations and some of the features described in Sec. IV (i.e., narrow width of the angular distribution, decrease of the multiplicity of the energetic light particle with increasing Z of the gating particle) is one in which the projectile begins to coalesce with the target and before equilibrium is reached the fast particle is emitted. The remainder of the projectile is then fused with the

target. Evaporation from the compound system returns the compound nucleus to an average mass that is similar to that of the target. This picture could also account for the phenomenological explanation of the data that shows the cross-section dependence on E and θ for light ions can be explained if they are emitted from a source with a velocity of approximately one-half that of the projectile velocity.[2,14,18,24,33] This could be the average velocity of the PLF, as it is in the process of fusing, at the time the energetic light ion is emitted.

VI. SUMMARY

The measurements reported here suggest that there are several reaction processes contributing to the nonequilibrium fast particle yields. Some energetic light ions are associated with a PLF. There are three observations that favor the conclusion that energetic light ions observed in coincidence with PLF's are emitted during the collision process and not sequentially: (1) the widths and peak positions of the light-ion angular distributions at most show very weak dependence on the energy of the projectile, on the energy of the emitted light ion, and on the Z of the gating PLF; (2) the experimental widths do not agree with the predictions of the computer program LILITA for the DIC; and (3) the multiplicity of energetic light ions obtained when gating on low- and high-energy light ions are genrally comparable. Points (1) and (3) indicate the coincident PLF has no memory of the emission of the energetic light ion.

Other energetic light ions are found in coincidence only with $Z=1,2$ particles, and the fraction increases with increasing light-ion energy. These conclusions are based on the observed dependence of the $Z=1,2$ multiplicities on the Z of the gating particle, and on the comparison of γ-ray multiplicity and distribution of residual nuclei to those calculated with the program LILITA. The variation in multiplicity of the alpha particles on the Z of the gating PLF's is suggestive of some breakup of the projectile. Coincidences of protons with C and of alpha particles with B and C demonstrate that some particles do not come from the projectile in a simple one-step process. There are some effects which may require still other (weaker) reaction processes; for example, the asymmetry in the 136-MeV data for the proton angular distributions and the peculiar minimum at 17° in the proton angular distribution for $E_{^{12}C}=194$ MeV observed when gating on B, C, and N.

The distribution of residual nuclei in coincidence with low-energy alpha particles is consistent with the complete fusion picture. However, those resulting from coincidences with high-energy alpha particles and low- and high-energy protons are supportive of a strong nonequilibrium process. Many of the observed features can be accounted for if the energetic light ion is emitted in the collision process when the projectile begins to coalesce with the target.

This research was supported by the Division of Basic Energy Sciences, U. S. Department of Energy, under Contract W-7405-eng-26 with the Union Carbide Corporation.

*Present address: Bell Laboratories, Indiana Hill, Warrenville-Naperville Road, Naperville, Illinois.

[1]D. K. Scott, Michigan State University Reports MSUCL-326 and MSUCL-337, 1980.
[2]T. J. M. Symons, P. Doll, M. Bini, D. L. Hendrie, J. Mahoney, G. Mantzouranis, D. K. Scott, K. Van Bibber, Y. P. Viyogi, H. H. Wieman, and C. K. Gelbke, Phys. Lett. 94B, 131 (1980).
[3]G. D. Westfall, J. Gosset, P. J. Johansen, A. M. Poskanzer, W. G. Meyer, H. H. Gutbrod, A. Sandoval, and R. Stock, Phys. Rev. Lett. 37, 1202 (1976); J. Gosset, H. H. Gutbrod, W. G. Meyers, A. M. Poskanzer, A. Sandoval, R. Stock and G. D. Westfall, Phys. Rev. C 16, 629 (1977).
[4]M. Blann, Nucl. Phys. A235, 211 (1974).
[5]J. J. Griffin, Phys. Lett. 24B, 5 (1967).
[6]H. W. Bertini, R. T. Santoro, and O. W. Hermann, Phys. Rev. C 14, 590 (1976).
[7]J. B. Ball, C. B. Fulmer, M. L. Mallory, and R. L. Robinson, Phys. Rev. Lett. 40, 1698 (1978).
[8]C. K. Gelbke, M. Bini, C. Olmer, D. L. Hendrie, J. L. Laville, J. Mahoney, M. C. Mermaz, D. K. Scott, and H. H. Wieman, Phys. Lett. 71B, 83 (1977).
[9]H. Ho, R. Albrecht, W. Dunnweber, G. Graw, S. G. Steadman, J. P. Wurm, D. Disdier, V. Rauch, and F. Scheibling, Z. Phys. A 283, 235 (1977).
[10]R. K. Bhowmik, E. C. Pollacco, N. E. Sanderson, J. B. A. England, and G. S. Morrison, Phys. Lett. 80B, 41 (1978).
[11]A. Gamp, J. C. Jacmart, N. Poffe, H. Doubre, J. C. Roynette, and J. Wilczynski, Phys. Lett. 74B, 215 (1978).

[12]M. Bini, C. K. Gelbke, D. K. Scott, T. J. M. Symons, P. Doll, D. L. Hendrie, J. L. Laville, J. Mahoney, M. C. Mermaz, C. Olmer, K. Van Bibber, and H. H. Wieman, Phys. Rev. C 22, 1945 (1980).
[13]G. R. Young, R. L. Ferguson, A. Gavron, D. C. Hensley. F. E. Obenshain, F. Plasil, A. H. Snell, M. P. Webb, C. F. Maguire, and G. A. Petitt, Phys. Rev. Lett. 45, 1389 (1980).
[14]A. Gavron, R. L. Ferguson, F. E. Obenshain, F. Plasil, G. R. Young, G. A. Petitt, K. Geoffroy Young, D. G. Sarantites, and C. F. Maguire, Phys. Rev. Lett. 46, 8 (1981).
[15]H. Gemmeke, P. Netter, A. Richter, L. Lassen, S. Lewandowski, W. Lucking, and R. Schreck, Phys. Lett. 97B, 213 (1980).
[16]R. P. Schmitt, G. J. Wozniak, G. V. Rattazzi, G. J. Mathews, R. Regimbart, and L. G. Moretto, Phys. Rev. Lett. 522 (1981).
[17]L. Westerberg, D. G. Sarantites, D. C. Hensley, R. A. Dayras, M. L. Halbert, and J. H. Barker, Phys. Rev. C 18, 796 (1978).
[18]K. Geoffroy Young, D. G. Sarantites, J. R. Beene, M. L. Halbert, D. C. Hensley, R. A. Dayras, and J. H. Barker, Phys. Rev. C, 23, 2479 (1981).
[19]A. Gavron, J. R. Beene, R. L. Ferguson, F. E. Obenshain, F. Plasil. G. R. Young, G. A. Petitt, K. Geoffroy Young, M. Jaaskelainen, D. G. Sarantites, and C. F. Maguire, Phys. Rev. C (to be published).
[20]K. Siwek-Wilczynska, E. H. du Marchie van Voorthuysen, J. van Popta, R. H. Siemssen, and J. Wilczynski, Phys. Rev. Lett. 42, 1599 (1979); Nucl. Phys. A330, 150 (1979).
[21]T. Inamura, M. Ishihara, T. Fukuda, T. Shimado, and H. Hiruta, Phys. Lett. 68B, 51 (1977).
[22]D. R. Zolnowski, H. Yamada, S. E. Cala, A. C. Kahler, and T. T. Sugihara, Phys. Rev. Lett. 41, 92 (1978).
[23]H. Yamada, D. R. Zolnowski, S. E. Cala, A. C. Kahler, J. Pierce, and T. T. Sugihara, Phys. Rev. Lett. 43, 605 (1979).
[24]T. C. Awes, C. K. Gelbke, G. Poggi, B. B. Back, B. Glagola, H. Breuer, V. E. Viola, Jr., and T. J. M. Symons, Phys. Rev. 45, 513 (1980).
[25]K. van Bibber, W. Pang, M. Avery, and E. Bloemhof, IEEE Trans. Nucl. Sci. 27, 86 (1980).
[26]G. B. Hagemann, R. Broda, B. Herskind, M. Ishihara, S. Ogaza, and H. Ryde, Nucl. Phys. A245, 166 (1975).
[27]S. Cohen, F. Plasil, and W. J. Swiatecki, Ann. Phys. (N. Y.) 82, 557 (1974).
[28]J. Wilczynski, Nucl. Phys. A216, 386 (1973).
[29]J. Gomez del Campo and R. G. Stokstad, ORNL Report TM-7295, 1981.
[30]D. Glas and U. Mosel, Nucl. Phys. A237, 429 (1975).
[31]R. A. Dayras, R. G. Stokstad, D. C. Hensley, M. L. Halbert, D. G. Sarantites, L. Westerberg, and J. H. Barker, Phys. Rev. C 22, 1485 (1980).
[32]J. Gomez del Campo, Proceedings of the Symposium on Heavy Ion Physics from 10 to 200 MeV/amu, edited by J. Barrette and P. D. Bond, BNL Report 51115, 1979, Vol. I, p. 93.
[33]R. L. Auble, J. B. Ball, F. E. Bertrand, R. L. Ferguson, C. B. Fulmer, I. Y. Lee, R. L. Robinson, G. R. Young, J. R. Wu, J. C. Wells, and H. Yamada (unpublished).